24. S. A. Zimov *et al.*, *Clim. Change* **33**, 111–120 (1996).
25. See section SM7 in the supplementary materials.
26. FRA, "Global Forest Resources Assessment 2010" (Food and Agriculture Organization of the United Nations, Rome, 2010).
27. G. C. Hurtt *et al.*, *Clim. Change* **109**, 117–161 (2011).
28. Y. Pan *et al.*, *Science* **333**, 988–993 (2011).
29. O. L. Phillips *et al.*, *Science* **323**, 1344–1347 (2009).
30. K. R. Gurney, W. J. Eckels, *Tellus B Chem. Phys. Meterol.* **63**, 328–339 (2011).
31. K. E. Taylor, R. J. Stouffer, G. A. Meehl, *Bull. Am. Meteorol. Soc.* **93**, 485–498 (2012).
32. See section SM9 in the supplementary materials.
33. A. D. McGuire *et al.*, *Global Biogeochem. Cycles* **15**, 183–206 (2001).
34. K. Schaefer *et al.*, *J. Geophys. Res.* **117**, G03010 (2012).
35. L. Rustad *et al.*, *Oecologia* **126**, 543–562 (2001).
36. R. A. Houghton, *J. Geophys. Res.* **92**, 4223 (1987).
37. G. H. Kohlmaier *et al.*, *Tellus B Chem. Phys. Meterol.* **41**, 487–510 (1989).
38. R. J. Norby *et al.*, *Proc. Natl. Acad. Sci. U.S.A.* **102**, 18052–18056 (2005).
39. P. D. Jones *et al.*, *J. Geophys. Res.* **117**, D05127 (2012).
40. J. Hansen, R. Ruedy, M. Sato, K. Lo, *Rev. Geophys.* **48**, RG4004 (2010).
41. G. R. Walther *et al.*, *Nature* **416**, 389–395 (2002).
42. S. C. Elmendorf *et al.*, *Nat. Clim. Change* **2**, 453–457 (2012).
43. K. E. N. Tape, M. Sturm, C. Racine, *Glob. Change Biol.* **12**, 686–702 (2006).
44. A. J. Soja *et al.*, *Global Planet. Change* **56**, 274–296 (2007).
45. E. S. Kasischke *et al.*, *Can. J. Res.* **40**, 1313–1324 (2010).
46. S. A. Zimov *et al.*, *Science* **284**, 1973–1976 (1999).
47. L. R. Welp, J. T. Randerson, H. P. Liu, *J. Geophys. Res.* **111**, G03007 (2006).
48. S. J. Goetz, A. G. Bunn, G. J. Fiske, R. A. Houghton, *Proc. Natl. Acad. Sci. U.S.A.* **102**, 13521–13525 (2005).
49. D. Verbyla, *Glob. Ecol. Biogeogr.* **17**, 547–555 (2008).
50. P. E. Thornton, J.-F. Lamarque, N. A. Rosenbloom, N. M. Mahowald, *Global Biogeochem. Cycles* **21**, GB4018 (2007).
51. P. P. Tans, I. Y. Fung, T. Takahashi, *Science* **247**, 1431–1438 (1990).
52. K. R. Gurney *et al.*, *Nature* **415**, 626–630 (2002).
53. B. B. Stephens *et al.*, *Science* **316**, 1732–1735 (2007).
54. C. D. Keeling, S. C. Piper, T. P. Whorf, R. F. Keeling, *Tellus B Chem. Phys. Meterol.* **63**, 1–22 (2011).
55. We specify the uncertainty in CO_2 amplitude with 95% confidence intervals estimated using a jackknife procedure (fig. S3).
56. Only two models' simulations extended to 2011 (HadGEM2-ES and NorESM-1). Other models' output was available only through 2005, so NEP for 2009 to 2011 is given by the mean over 2001 to 2005. In these models, the change in NEP amplitude up to 2001 to 2005 may be 10% smaller than the change up to 2009 to 2011.

Acknowledgments: The Scripps CO_2 Program is supported by DOE grant DE-SC0005090. HIPPO was supported by NSF grants ATM-0628575, ATM-0628519, ATM-0628388, ATM-0628452, and ATM-1036399, and by the National Center for Atmospheric Research (NCAR). Recovery and updating of early aircraft, MLO, and BRW data was supported by NSF grant ATM-1036399. L.R.W. was supported by NASA award NNX11AF36G. Early observations at BRW were funded by U.S. Navy/Office of Naval Research contract N00014-67-A-0103-0007. Online access to all observational data is summarized in section SM10 of the supplementary materials. NCAR is supported by the NSF. Any opinions, findings, and conclusions or recommendations expressed in this material are those of the authors and do not necessarily reflect the views of NOAA, NSF, DOE or NASA. We thank the HIPPO science team and the crew and support staff at the NCAR Research Aviation Facility. We acknowledge the World Climate Research Programme's Working Group on Coupled Modelling, which is responsible for CMIP, and we thank the climate modeling groups for producing and making available their model output. Support of the CMIP data sets is provided by the Office of Science, U.S. Department of Energy. C. Roedenbeck provided assistance with the TM3 model. P.K.P. is partially supported by the Ministry of Education, Culture, Sports, Science and Technology Green Network of Excellence program. G.W.S. acknowledges support from the NSF Graduate Research Fellowship Program and the Environmental Protection Agency's Science to Achieve Results program.

Supplementary Materials

www.sciencemag.org/cgi/content/full/science.1239207/DC1
Materials and Methods
Figs. S1 to S9
Tables S1 to S7
References (*57*–*81*)

16 April 2013; accepted 17 July 2013
Published online 8 August 2013;
10.1126/science.1239207

Expanding the Fluorine Chemistry of Living Systems Using Engineered Polyketide Synthase Pathways

Mark C. Walker,[1]* Benjamin W. Thuronyi,[2]* Louise K. Charkoudian,[3]† Brian Lowry,[4] Chaitan Khosla,[3,4,5] Michelle C. Y. Chang[1,2]‡

Organofluorines represent a rapidly expanding proportion of molecules that are used in pharmaceuticals, diagnostics, agrochemicals, and materials. Despite the prevalence of fluorine in synthetic compounds, the known biological scope is limited to a single pathway that produces fluoroacetate. Here, we demonstrate that this pathway can be exploited as a source of fluorinated building blocks for introduction of fluorine into natural-product scaffolds. Specifically, we have constructed pathways involving two polyketide synthase systems, and we show that fluoroacetate can be used to incorporate fluorine into the polyketide backbone in vitro. We further show that fluorine can be inserted site-selectively and introduced into polyketide products in vivo. These results highlight the prospects for the production of complex fluorinated natural products using synthetic biology.

The catalytic diversity of biological systems provides enormous potential for application of living cells to the scalable production of pharmaceuticals, fuels, and materials (*1*–*4*). However, the scope of innovation of living organisms is typically limited to functions that confer a direct advantage for cell growth, thereby maximizing biomass as the end product rather than a distinct molecule or reaction of interest. In contrast, synthetic biology approaches allow us to disconnect some of these biochemical transformations from cell survival and reconnect them in different ways for the targeted synthesis of alternative classes of compounds. One particularly interesting area of opportunity is the development of methods to introduce fluorine into complex small-molecule scaffolds, which has become a powerful strategy for the design of synthetic pharmaceuticals. Estimates indicate that 20 to 30% of drugs, including many of the top sellers, contain at least one fluorine atom (*5*–*7*). Recent innovations have expanded the scope of synthetic C–F bond-forming methodologies, but the unusual elemental properties of fluorine that serve as the basis for its success also continue to restrict the range of molecular structures that can be accessed (*8*–*11*). As such, the invention of alternative routes for the site-selective introduction of fluorine into structurally diverse molecules, particularly under mild conditions, remains an outstanding challenge.

In comparison to synthetic small molecules, fluorine has limited distribution in naturally occurring organic compounds; the only organofluorine natural products characterized to date consist of a small set of simple molecules associated with the fluoroacetate pathway of *Streptomyces cattleya*, a soil bacterium that has the ability to catalyze the formation of C–F bonds from aqueous fluoride (Fig. 1A) (*12*, *13*). Although these compounds lack the intricacy typically expected of secondary metabolites, they represent a potentially rich source of modular organofluorine building blocks for the production of complex fluorinated natural products. In this regard, the backbones of several large classes of medicinally relevant natural products—including polyketides, isoprenoids, steroids, alkaloids, eicosanoids, leukotrienes, and others—are biosynthesized directly from the assembly and tailoring of simple acetate units (Fig. 1A). Introduction of the fluoroacetate monomer in place of acetate would allow us to incorporate fluorine into the backbone of these targets and create new molecular function by combining the medicinal

[1]Department of Molecular and Cell Biology, University of California, Berkeley, Berkeley, CA 94720–1460, USA. [2]Department of Chemistry, University of California, Berkeley, Berkeley, CA 94720–1460, USA. [3]Department of Chemistry, Stanford University, Stanford, CA 94305, USA. [4]Department of Chemical Engineering, Stanford University, Stanford, CA 94305, USA. [5]Department of Biochemistry, Stanford University, Stanford, CA 94305, USA.

*These authors contributed equally to this work.
†Present address: Department of Chemistry, Haverford College, Haverford, PA 19041, USA.
‡Corresponding author. E-mail: mcchang@berkeley.edu

chemistry advantages of fluorine with the structural complexity and bioactivity of natural products. For example, the introduction of fluorine via synthetic or semisynthetic routes has enabled the improvement of the clinical properties of several natural products, but this remains challenging to achieve (*14*–*17*). Although previous studies have shown that distal fluorine substituents can be accommodated in natural-product biosynthetic pathways (*18*, *19*), access to fluoromalonyl–coenzyme A (CoA), a fluorinated analog of one of nature's most powerful carbon nucleophiles, as an extender unit would enable a general method for direct incorporation of fluorine into any polyketide structure.

Many acetate-based natural products, polyketides in particular, are generated through the iterative condensation of activated thioesters, resulting in reactive β-keto units that condense further to produce a wide range of structures (*20*, *21*) (Fig. 1B). The structural diversity of polyketides is especially notable given that the majority of polyketides draw on only two monomers, acetate and propionate, as the extender units that form their carbon skeletons (*3*, *20*, *22*). Although polyketide synthases (PKSs) have been observed to be accommodating with regard to their starter units (*23*), the encoding of extender units has been found to be quite selective, and many cellular acyl-CoAs are excluded from the backbone (*22*). However, progress in engineering extender-unit incorporation has been made by domain engineering (*23*–*25*) or incorporation via a domain that encodes a rare extender unit (*17*, *26*). Although fluoroacetate serves as a starter unit in nature to produce highly toxic ω-fluoro fatty acids (Fig. 1A) (*13*), fluorine has never been observed to date within the backbone, implying that chain-extension reactions with the fluorinated acyl-CoA do not occur in these systems. The apparent inability of living systems to use fluoroacetate for the biosynthesis of complex small molecules probably results in part from the extreme properties of fluorine that affect biological and chemical synthesis. For example, the pK_a (where K_a is the acid dissociation constant) of the α proton, electrophilicity of the carbonyl group, and the stability of the acyl-CoA and its corresponding carbanion are all highly affected by fluorine substitution. Furthermore, the fluoroacetyl group bears a clear similarity to the fluoromethylketone motif used for the design of covalent inhibitors, suggesting that the irreversible alkylation of active-site nucleophiles could also create problems (*27*). Thus, the development of a system to incorporate fluorinated extender units could dramatically increase the range of complex structures that can be accessed but must also address the challenges in activating the fluoroacetate monomer for the downstream C–C bond-forming chemistry involved in chain-extension reactions.

Chain elongation in polyketides and related fatty acid–based natural products relies on a separate pool of extender units formed by carboxylation of acyl-CoAs at the α position. These malonyl-CoA derivatives are then used as masked enolates for C–C bond formation after decarboxylation. The fluorinated extender, fluoromalonyl-CoA, can be made through two routes: either (i) a two-step activation of the biogenic fluoroacetate or (ii) a direct ligation of CoA to fluoromalonate (Fig. 2). We reasoned that the acetate kinase (AckA)–phosphotransacetylase (Pta) pair would be effective at fluoroacetate activation, as mutations in this gene locus have been shown to lead to fluoroacetate resistance in *Escherichia coli* (*28*). The enzymes from *E. coli* were overexpressed and characterized biochemically, confirming that AckA

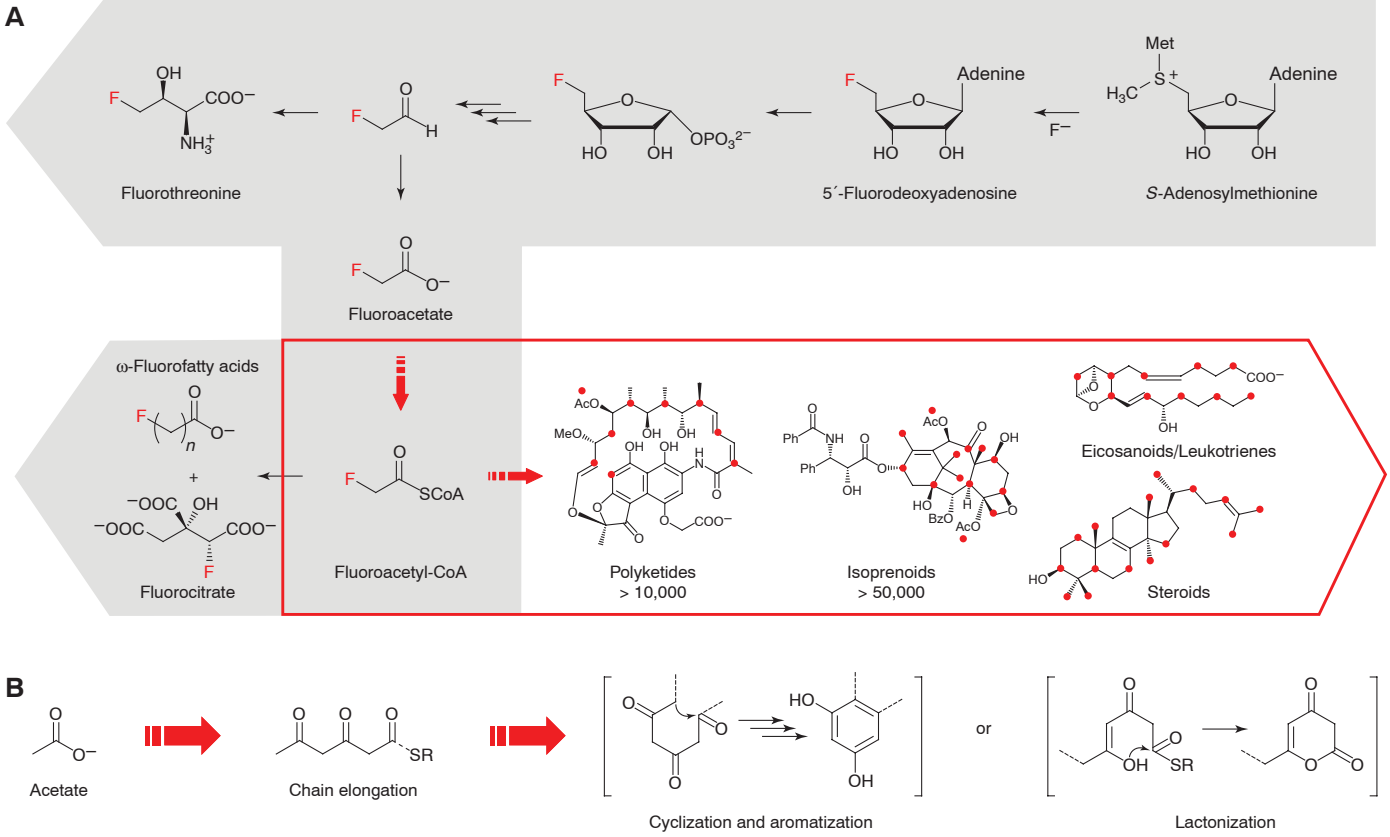

Fig. 1. Synthetic biology of fluorine. (**A**) The fluoroacetate pathway and its metabolites represent the known scope of biological fluorine chemistry, starting with fluoride and *S*-adenosylmethionine, to produce fluoroacetate and fluorothreonine as the end products (right to left, gray box). This scope could be greatly expanded by engineering downstream pathways to use fluoroacetate as a building block for site-selective introduction of fluorine into large families of natural products constructed from acetate backbones (left to right, red box). Red dots represent positions that could, in principle, be fluorinated by incorporation of a fluoroacetate monomer without altering the carbon skeleton, including locations where fluorine would replace a methyl group derived from propionate or where downstream tailoring steps have occurred on the final structure. (**B**) Assembly of acetate units in the biosynthesis of polyketide natural products. R, CoA or PKS.

and Pta serve as an effective activation system to rapidly produce both acetyl- and fluoroacetyl-CoA in nearly quantitative yield (figs. S1 and S2). Analysis of the kinetic parameters for these enzymes with respect to fluorinated substrates indicated that neither appears to be affected by the fluorine substituent beyond inductive effects that alter the nucleophilicity of the carboxylic acid (AckA) or electrophilicity of the carbonyl (Pta) (*29*). Next, we purified the individual AccABCD subunits that make up the acetyl-CoA carboxylase (ACCase) from *E. coli* and added these enzymes to the AckA-Pta system to carry out the carboxylation of fluoroacetate in a one-pot reaction to generate the fluoromalonyl-CoA extender unit (Fig. 2A and fig. S1). Under these conditions, the ligation of CoA by AckA-Pta to produce the acyl-CoA is rapid, and production of the carboxylated product is limited by the ACCase. Although the rate of conversion is 4.5 times slower for fluoroacetate as compared with acetate, the overall extent of reaction is similar for both congeners, which suggests that covalent inactivation of the ACCase by fluoroacetyl-CoA is not important if it occurs. In addition to the route from fluoroacetate, we also tested a malonyl-CoA synthetase (MatB) (*30*) for coupling CoA directly to fluoromalonate. Although MatB exhibits a 10^3-fold selectivity for malonate over fluoromalonate, fluoromalonyl-CoA is still produced at reasonable efficiency (Fig. 2B and figs. S3 and S4). Both of these systems also provide in situ regeneration capacity that can amplify product yields from polyketide synthases, and we found that either system increased polyketide production by tetrahydroxynaphthalene synthase (*31*) compared with simple addition of malonyl-CoA (fig. S5).

We next turned our attention to the use of the fluoromalonyl-CoA monomer for downstream chain-elongation reactions. To start, we examined the behavior of a simple polyketide synthase system with regard to one cycle of chain extension and ketoreduction, which is a key functionality of larger multimodular systems for controlling downstream cyclization and rearrangements within the polyketide backbone (Fig. 3A) (*3*, *20*). We constructed a synthetic gene encoding NphT7 (*32*), which appears to be a free-standing ketosynthase that is related at the structural level to the ketosynthase domain of more complex polyketide synthases (fig. S6), and we isolated the heterologously expressed enzyme for biochemical characterization (fig. S1). With the use of a coupled assay with an *R*-hydroxyl forming acetoacetyl-CoA reductase (PhaB), we found that NphT7 is competent to catalyze the formation of acetofluoroacetyl-CoA, using an acetyl-CoA starter and fluoromalonyl-CoA extender with only a five-fold defect in catalytic efficiency (k_{cat}/K_M, where k_{cat} is the turnover rate and K_m is the Michaelis constant) derived from a drop in k_{cat} with the fluorinated substrate (Fig. 3). This lower turnover rate observed with the fluorinated substrate is possibly related to the reduced reactivity of the enolate species, which would be stabilized by the fluorine substituent. However, the overall yield was comparable for both fluorinated and nonfluorinated substrates, which shows that a decarboxylative Claisen condensation with fluoromalonyl-CoA can take place at a similar extent of conversion compared to malonyl-CoA. Furthermore, these experiments also show that the 2-fluoro-3-keto motif produced with the fluoromalonyl-CoA extender can be accepted by ketoreductases, as PhaB is capable of efficiently reducing the acetofluoroacetyl-CoA substrate (fig. S7). The ^{1}H and ^{19}F nuclear magnetic resonance (NMR) spectra of the reduced product indicate that both diastereomers are produced in this reaction (fig. S7), which may result from lack of stereochemical preference of NphT7 with respect to the fluorine substituent or from racemization of the product before reduction by PhaB. Although PhaB does not appear to show diastereoselectivity with respect to the fluorine group, the polyketide synthase ketoreductases are known to be selective with regard to their native α substituent and could potentially carry out the stereochemical resolution of the fluorine modification upon reduction (*33*).

With this information in hand, we sought to extend our biosynthetic method for fluorine introduction to more complex polyketide synthase systems, which use the chain-elongation reaction for the biosynthesis of many bioactive and clinically important natural products, such as erythromycin and rapamycin (*3*, *20*). Of the multimodular polyketide systems, 6-deoxyerythronolide B synthase (DEBS) is probably the best understood and is responsible for production of the erythromycin precursor (*34*). We therefore focused our studies on the sixth module of DEBS, including the terminal thioesterase ($DEBS_{Mod6}$+TE) (*35*). Using a diketide substrate [natural diketide *N*-acetyl cysteamine thioester (NDK-SNAC)], $DEBS_{Mod6}$+TE can catalyze a single round of chain elongation with its native methylmalonyl-CoA extender unit and then cyclize the tethered product to form a methyltriketide lactone (TKL) (Fig. 4A, R = CH_3; Fig. 4B, **1**; and fig. S8) (*36*). We found that $DEBS_{Mod6}$+TE is also able to accept the fluorinated monomer in chain-extension catalysis to form the 2-fluoro-2-desmethyltriketide lactone (F-TKL) and incorporate fluorine into the polyketide backbone (Fig. 4B, **2** to **4**; and fig. S9). The identity of the F-TKL was established by comparison to an authentic synthetic standard using reverse-phase liquid chromatography–mass spectrometry (LC-MS) monitored by electrospray ionization (ESI) and further confirmed by characterization of the isolated compound by high-resolution MS, gas chromatography–mass spectrometry, and ^{19}F NMR spectroscopy (figs. S10 to S13). Although the

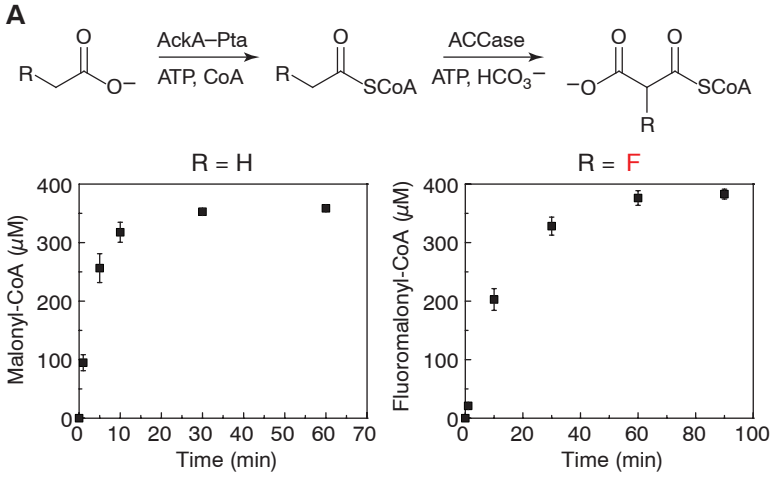

	R =	k_{cat} (s^{-1})	K_M (μM)	k_{cat}/K_M ($M^{-1}s^{-1}$)
Malonate	H	11.8 ± 0.3	71 ± 5	(1.7 ± 0.1) x 10^5
Methylmalonate	CH_3	1.49 ± 0.02	38 ± 2	(3.9 ± 0.2) x 10^4
Fluoromalonate	F	0.29 ± 0.01	550 ± 40	(5.3 ± 0.4) x 10^2

Fig. 2. Enzymatic production of activated extender units for C–C bond-formation reactions. (A) Formation of malonyl-CoA (left) and fluoromalonyl-CoA (right) from 500 μM CoA and either acetate or fluoroacetate, respectively. Values are reported as the mean ± SD (n = 3 replicates). **(B)** Kinetic parameters for malonate activation. Kinetic parameters are reported as mean ± SE (n = 3), as determined from nonlinear curve-fitting. Error in the k_{cat}/K_M parameter was obtained from propagation of error from the individual kinetic terms.

2*S* keto tautomer is generated in ≥94% diastereomeric excess (figs. S12 and S13), this ratio appears to be set by the compound's stereoelectronic factors rather than the stereochemical preference of DEBS$_{Mod6}$+TE, as the F-TKL is fully enolized in aqueous solution. The F-TKL can also be produced directly from fluoroacetate using the AckA-Pta/ACCase activation system in either a multistage (Fig. 4B, **5** and **6**) or single-pot reaction (Fig. 4B, **7** and **8**) with DEBS$_{Mod6}$+TE in a similar yield to the MatB reaction, which allows us to connect fluorinated polyketide production directly to the biosynthetically available fluorinated building block (Fig. 1A and scheme S1).

In contrast to the chain-extension reaction catalyzed by NphT7, DEBS$_{Mod6}$+TE does not incorporate fluorinated extender units into the triketide lactone product as efficiently as its native methylmalonyl-CoA extender. Preliminary studies indicate that the reduced efficiency of DEBS$_{Mod6}$+TE with the fluorinated extender is not due to covalent inactivation of the enzyme (fig. S14), but rather to the more complex biochemistry of polyketide synthases with regard to monomer selection (*37*). Extender unit hydrolysis, which occurs even for the native substrate (table S2), appears to limit fluoromalonyl-CoA incorporation based on the observations that MatB and adenosine triphosphate (ATP) are needed for fluoromalonyl-CoA regeneration and that fluoromalonate remains the major organofluorine species, even in their presence (fig. S15). The fluoromalonyl-CoA extender is, however, incorporated at higher efficiency by DEBS$_{Mod6}$+TE than malonyl-CoA (R = H), which is reported to be naturally excluded by DEBS (*38*). In fact, DEBS$_{Mod6}$+TE produces at least 10 times more F-TKL than H-TKL in a direct competition experiment with equimolar amounts (1 mM) of fluoromalonyl-CoA and malonyl-CoA (table S3).

To address the issue of site- or regioselective fluorine incorporation, we turned our attention to exploiting the greater reactivity of the fluorinated extender unit toward acylation reactions. In this regard, we hypothesized that it would be possible for a fluorinated substrate to selectively acylate either the acyltransferase (AT) or acyl carrier protein domains of individual DEBS modules in the presence of a catalytically compromised or inactive AT domain, an approach that has been shown to facilitate malonyl incorporation by DEBS (*39*). Experiments with DEBS$_{Mod6}$+TE showed that not only does F-TKL yield increase as expected, but fluorine selectivity also improves upon introduction of a key S2107A (Ser^{2107}→Ala^{2107}) mutation, reversing the selectivity of the wild-type module (Fig. 4C). When the NDK-SNAC substrate is used with its native module, DEBS$_{Mod2}$, in conjunction with the analogous S2652A mutation, extension with fluoromalonyl-CoA to form F-TKL reaches 30% efficiency compared with methylmalonyl-CoA (fig. S16). Furthermore, we found that the stand-alone trans-AT from the disorazole polyketide synthase (*40*, *41*) accepts fluoromalonyl-CoA and can further enhance F-TKL formation by the AT-null mutant (Fig. 4C). Using this approach, we began to explore the possibility of site-selective fluorine incorporation with a mini-PKS model system, consisting of DEBS$_{Mod2}$ and DEBS$_{Mod3}$+TE, that was designed to carry out two chain-extension reactions from the NDK-SNAC substrate (*42*). Using the appropriate AT-null constructs, we were able to observe exclusive production of either regioisomer of the fluoro-methyl tetraketide lactone (tetraKL). The identity of the 2-fluoro-4-methyl tetraKL and 2-methyl-4-fluoro tetraKL was established by both high-resolution ESI-MS and LC-MS on the basis of their different retention times, as well as their mass fragmentation patterns, which are consistent with the incorporation of fluorine at the expected sites (Fig. 4D and fig. S17). These studies also indicate that further chain extension after fluorine insertion can be achieved and that fluorinated intermediates could potentially be tolerated in downstream reactions. This observation is consistent with previous work that has shown that intermediates with non-native substituents, including fluorine, can be extended and tailored to the final structure (*3*, *17*–*20*, *23*) and gives promise that larger fluorinated polyketide targets may be accessible through this approach.

The observed selectivity for fluoromalonyl- over malonyl-CoA extender units suggests that polyketide chain-extension reactions with fluoromalonyl-CoA could possibly be catalyzed in vivo in *E. coli*, which contains a sizable malonyl-CoA pool (~35 μM) (*43*) but almost no methylmalonyl-CoA (*44*, *45*). We carried out preliminary ^{19}F-NMR studies of cells expressing MatB, NphT7, and PhaB and fed with nontoxic levels of fluoromalonate. Analysis of the media and cell extracts indicated that flux through fluoromalonyl-CoA could reach 100 μM to 1 mM, which is sufficient for use by PKSs in live cells (table S4). Next, we tested the ability of DEBS$_{Mod6}$+TE to catalyze chain elongation in cell lysates prepared from *E. coli* BAP1 coexpressing DEBS$_{Mod6}$+TE and MatB. Under these conditions, F-TKL is produced with no observable H-TKL upon addition of only NDK-SNAC, fluoromalonate, CoA, ATP, and the ATP regeneration system (fig. S18A). Negative controls with either no DEBS$_{Mod6}$+TE/MatB expressed or no NDK-SNAC substrate show no production of F-TKL (fig. S18A). These results demonstrate that the intracellular level of expression of the DEBS$_{Mod6}$+TE and MatB enzymes is sufficient for the incorporation of the fluorinated extender unit. They also further imply that fluorine could be introduced into the polyketide backbone inside living cells, which are capable of generating ATP through normal metabolic processes. Therefore, we cultured *E. coli* BAP1 coexpressing DEBS$_{Mod6}$+TE and MatB and harvested the cells after induction. These cells were then fed with the fluoromalonate precursor, which resulted in the production of F-TKL upon addition of NDK-SNAC (Fig. 4B, **9**; and fig. S18B). The identity of the F-TKL under these conditions was established by LC-MS, co-injection with an

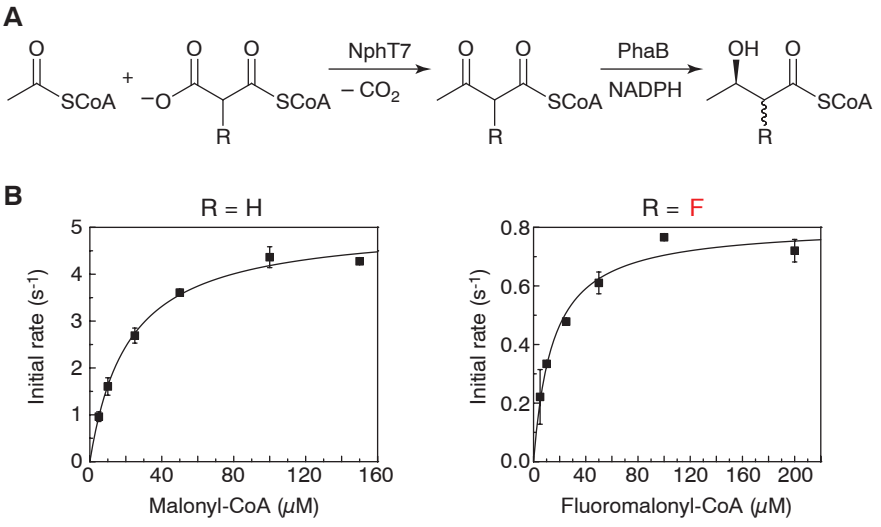

	R =	k_{cat} (s^{-1})	K_M (μM)	k_{cat}/K_M ($M^{-1}s^{-1}$)
Malonyl-CoA	H	5.1 ± 0.1	21 ± 2	(2.4 ± 0.2) x 10^5
Fluoromalonyl-CoA	F	0.81 ± 0.03	15 ± 2	(5.4 ± 0.7) x 10^4

Fig. 3. A chain-extension and ketoreduction cycle with a fluorinated extender using a simple polyketide synthase, NphT7. (**A**) Reactions catalyzed by NphT7 and PhaB. NADPH, reduced form of nicotinamide adenine dinucleotide phosphate. (**B**) Steady-state kinetic parameters for NphT7-catalyzed C–C bond formation measured using a coupled assay with PhaB. Data points are reported as the mean ± SD (n = 3). Kinetic parameters are reported as mean ± SE (n = 3), as determined from nonlinear curve-fitting. Error in the k_{cat}/K_M parameter was obtained from propagation of error from the individual kinetic terms.

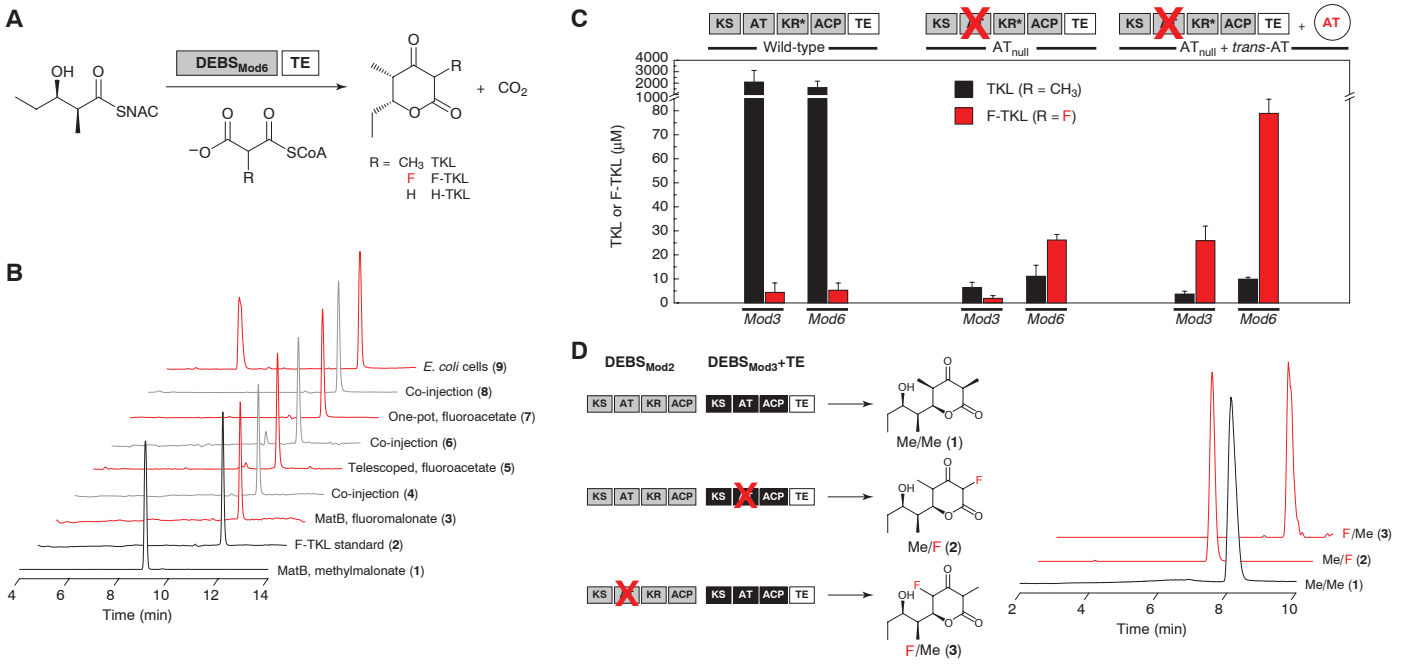

Fig. 4. Production of fluorinated polyketides in vitro and in vivo. (**A**) Reaction catalyzed by DEBS$_{Mod6}$+TE using the NDK-SNAC substrate with various extender units (NDK-SNAC, (2*S*,3*R*)-2-methyl-3-hydroxypentanoyl-*N*-acetylcysteamine thioester). (**B**) Chain extension by DEBS$_{Mod6}$+TE to form triketide lactones monitored by LC-MS [TKL, mass/charge ratio (*m/z*) = 169; F-TKL, *m/z* = 173]. CoA, ATP, and ATP regeneration system are included in all in vitro reactions. Data are normalized with respect to the TKL peak. (**C**) Selectivity of DEBS$_{Mod6}$+TE and DEBS$_{Mod3}$+TE for the methylmalonyl-CoA versus fluoromalonyl-CoA extender unit, as monitored by TKL (*m/z* = 169) and F-TKL (*m/z* = 173) formation. Conditions include wild-type modules, AT^0 modules, and AT^0 modules in conjunction with the trans-AT from the disorazole PKS (DszsAT). Values are reported as the mean ± SD (*n* = 3). KR* denotes that the KR domain of Mod3 is inactive. (**D**) LC-MS traces showing regioselective tetraketide lactone formation using the DEBS mini-PKS consisting of DEBS$_{Mod2}$ and DEBS$_{Mod3}$+TE (Me/Me, 2-methyl-4-methyl-tetraketide lactone, *m/z* = 227; Me/F, 2-fluoro-4-methyl-tetraketide lactone, *m/z* = 231; F/Me, 2-methyl-4-fluoro-tetraketide lactone, *m/z* = 231). Me/Me was produced using DEBS$_{Mod2}$/DEBS$_{Mod3}$+TE and methylmalonate (**1**). Me/F was produced using DEBS$_{Mod2}$/DEBS$_{Mod3}$AT^0+TE, DszsAT, methylmalonyl-CoA, and fluoromalonate (**2**). F/Me was produced using DEBS$_{Mod2}$AT^0/DEBS$_{Mod3}$+TE, methylmalonyl-CoA, and fluoromalonate (**3**). Data are normalized with respect to the Me/Me peak. All reactions contained MatB and the ATP regeneration system.

authentic standard, as well as high-resolution MS. Moreover, F-TKL can also be produced directly in cell culture with the simple addition of a mixture of both substrates to the media after induction of DEBS$_{Mod6}$+TE and MatB (fig. S18C). Taken together, these studies show that the natural selectivity of the polyketide synthase allows for the site-selective introduction of fluorine over hydrogen into the polyketide backbone inside living cells.

Using engineered pathways to link simple biogenic organofluorine building blocks into more complex fluorinated small-molecule targets, we have demonstrated that we can expand the fluorine chemistry of living systems. Because of the modular nature of the biosynthetic pathways used to produce polyketides and related acetate-derived natural products, these findings open the door to general strategies for exploring the fluorine synthetic biology of complex natural products.

References and Notes

1. D. K. Ro *et al.*, *Nature* **440**, 940–943 (2006).
2. S. Atsumi, T. Hanai, J. C. Liao, *Nature* **451**, 86–89 (2008).
3. D. E. Cane, C. T. Walsh, C. Khosla, *Science* **282**, 63–68 (1998).
4. A. M. Weeks, M. C. Y. Chang, *Biochemistry* **50**, 5404–5418 (2011).
5. K. Müller, C. Faeh, F. Diederich, *Science* **317**, 1881–1886 (2007).
6. D. O'Hagan, *Chem. Soc. Rev.* **37**, 308–319 (2008).
7. T. Furuya, A. S. Kamlet, T. Ritter, *Nature* **473**, 470–477 (2011).
8. N. D. Ball, M. S. Sanford, *J. Am. Chem. Soc.* **131**, 3796–3797 (2009).
9. D. A. Watson *et al.*, *Science* **325**, 1661–1664 (2009).
10. V. Rauniyar, A. D. Lackner, G. L. Hamilton, F. D. Toste, *Science* **334**, 1681–1684 (2011).
11. E. Lee *et al.*, *Science* **334**, 639–642 (2011).
12. C. Dong *et al.*, *Nature* **427**, 561–565 (2004).
13. D. O'Hagan, *J. Fluor. Chem.* **127**, 1479–1483 (2006).
14. A. Rivkin, K. Biswas, T.-C. Chou, S. J. Danishefsky, *Org. Lett.* **4**, 4081–4084 (2002).
15. J.-P. Bégué, D. Bonnet-Delpon, *J. Fluor. Chem.* **127**, 992–1012 (2006).
16. B. Llano-Sotelo *et al.*, *Antimicrob. Agents Chemother.* **54**, 4961–4970 (2010).
17. S. Mo *et al.*, *J. Am. Chem. Soc.* **133**, 976–985 (2011).
18. W. Rungunphan, J. J. Maresh, S. E. O'Connor, *Proc. Natl. Acad. Sci. U.S.A.* **106**, 13673–13678 (2009).
19. R. J. M. Goss *et al.*, *ChemBioChem* **11**, 698–702 (2010).
20. J. Staunton, K. J. Weissman, *Nat. Prod. Rep.* **18**, 380–416 (2001).
21. R. Croteau, T. M. Kutchan, N. G. Lewis, in *Biochemistry and Molecular Biology of Plants*, R. B. Buchanan, W. Gruissem, R. Jones, Eds. (American Society of Plant Biologists, Rockville, MD, 2000), pp. 1250–1318.
22. Y. A. Chan, A. M. Podevels, B. M. Kevany, M. G. Thomas, *Nat. Prod. Rep.* **26**, 90–114 (2009).
23. R. McDaniel *et al.*, *Proc. Natl. Acad. Sci. U.S.A.* **96**, 1846–1851 (1999).
24. U. Sundermann *et al.*, *ACS Chem. Biol.* **8**, 443–450 (2013).
25. I. Koryakina, J. B. McArthur, M. M. Draelos, G. J. Williams, *Org. Biomol. Chem.* **11**, 4449–4458 (2013).
26. A. S. Eustáquio, D. O'Hagan, B. S. Moore, *J. Nat. Prod.* **73**, 378–382 (2010).
27. J. C. Powers, J. L. Asgian, Ö. D. Ekici, K. E. James, *Chem. Rev.* **102**, 4639–4750 (2002).
28. T. D. K. Brown, M. C. Jones-Mortimer, H. L. Kornberg, *J. Gen. Microbiol.* **102**, 327–336 (1977).
29. M. C. Walker, M. Wen, A. M. Weeks, M. C. Y. Chang, *ACS Chem. Biol.* **7**, 1576–1585 (2012).
30. A. J. Hughes, A. Keatinge-Clay, *Chem. Biol.* **18**, 165–176 (2011).
31. M. Izumikawa *et al.*, *J. Ind. Microbiol. Biotechnol.* **30**, 510–515 (2003).
32. E. Okamura, T. Tomita, R. Sawa, M. Nishiyama, T. Kuzuyama, *Proc. Natl. Acad. Sci. U.S.A.* **107**, 11265–11270 (2010).
33. A. P. Siskos *et al.*, *Chem. Biol.* **12**, 1145–1153 (2005).
34. C. Khosla, Y. Tang, A. Y. Chen, N. A. Schnarr, D. E. Cane, *Annu. Rev. Biochem.* **76**, 195–221 (2007).
35. R. S. Gokhale, S. Y. Tsuji, D. E. Cane, C. Khosla, *Science* **284**, 482–485 (1999).
36. N. Wu, F. Kudo, D. E. Cane, C. Khosla, *J. Am. Chem. Soc.* **122**, 4847–4852 (2000).
37. S. A. Bonnett *et al.*, *Chem. Biol.* **18**, 1075–1081 (2011).
38. G. F. Liou, J. Lau, D. E. Cane, C. Khosla, *Biochemistry* **42**, 200–207 (2003).
39. P. Kumar, A. T. Koppisch, D. E. Cane, C. Khosla, *J. Am. Chem. Soc.* **125**, 14307–14312 (2003).
40. F. T. Wong, A. Y. Chen, D. E. Cane, C. Khosla, *Biochemistry* **49**, 95–102 (2010).
41. F. T. Wong, X. Jin, I. I. Mathews, D. E. Cane, C. Khosla, *Biochemistry* **50**, 6539–6548 (2011).
42. S. Y. Tsuji, D. E. Cane, C. Khosla, *Biochemistry* **40**, 2326–2331 (2001).

43. B. D. Bennett *et al.*, *Nat. Chem. Biol.* **5**, 593–599 (2009).
44. T. Haller, T. Buckel, J. Rétey, J. A. Gerlt, *Biochemistry* **39**, 4622–4629 (2000).
45. B. A. Pfeifer, S. J. Admiraal, H. Gramajo, D. E. Cane, C. Khosla, *Science* **291**, 1790–1792 (2001).

Acknowledgments: We thank B. Bond-Watts and I. Aanei for assembly and cloning of the synthetic *nphT7* gene, X. Yu for providing plasmids for the *E. coli* ACCase, C. Harvey for synthetic chemistry assistance, F. T. Wong for helpful discussions, and A. Lingel (Novartis) for QCI-F CryoProbe use. The College of Chemistry NMR Facility at the University of California, Berkeley (UC Berkeley) is supported in part by the NIH (grants 1S10RR023679-01 and S10 RR16634-01). M.C.W. and B.W.T acknowledge the support of a NIH National Research Service Award Training Grant (1 T32 GMO66698) and the Gerald K. Branch Predoctoral Fellowship and UC Cancer Research Council Committee Predoctoral Fellowship (to B.W.T). L.K.C. acknowledges support from the National Cancer Institute (grant F32 CA137994). This work was funded by generous support from UC Berkeley and the NIH (grant 1 DP2 OD008696 to M.C.Y.C. and grant R01 GM087934 to C.K.).

Supplementary Materials
www.sciencemag.org/cgi/content/full/341/6150/1089/DC1
Materials and Methods
Figs. S1 to S18
Tables S1 to S4
Scheme S1
References (*46*–*60*)

24 June 2013; accepted 5 August 2013
10.1126/science.1242345

Observation of Partial Wave Resonances in Low-Energy O_2–H_2 Inelastic Collisions

Simon Chefdeville,[1,2] Yulia Kalugina,[3,4] Sebastiaan Y. T. van de Meerakker,[5] Christian Naulin,[1,2] François Lique,[3]* Michel Costes[1,2]*

Partial wave resonances predicted to occur in bimolecular collision processes have proven challenging to observe experimentally. Here, we report crossed-beam experiments and quantum-scattering calculations on inelastic collisions between ground-state O_2 and H_2 molecules that provide state-to-state cross sections for rotational excitation of O_2 (rotational state $N = 1$, $j = 0$) to O_2 ($N = 1$, $j = 1$) in the vicinity of the thermodynamic threshold at 3.96 centimeter^{-1}. The close agreement between experimental and theoretical results confirms the classically forbidden character of this collision-induced transition, which occurs exclusively in a purely quantum mechanical regime via shape and Feshbach resonances arising from partial waves with total angular momentum (J) = 2 to 4.

The accurate description of collisions between individual molecules remains a long-standing goal in physical chemistry. In a classical picture, the outcome of a collision is determined by the interaction potential and initial conditions such as relative velocity and impact parameter, that is, the distance of closest approach between the molecules in the absence of any interaction. Surely, molecules are quantum objects in nature, and the collisions must be described in terms of interfering quantum-scattering states, or partial waves, instead. Each partial wave is the quantum mechanical analog of a classical trajectory with a given impact parameter and is characterized by a definite value of total angular momentum, J, which is conserved throughout the collision (*1*).

The contribution of individual partial waves to the scattering cross sections constitutes the ultimate information that can be obtained about a collision event. Whereas molecular scattering processes are nowadays described successfully by quantum mechanical methods throughout, the direct observation of individual partial waves in molecular collision experiments remains highly challenging. In fact, partial waves can only be distinguished when giving rise to scattering resonances that manifest as resolved peaks in differential or integral cross sections (DCSs and ICSs) as measured in crossed-beam experiments. Such very rare findings then provide a unique insight in the most critical part of the potential energy surface (PES), the transition state region (*2*). However, in most cases, the collision energy spread and the participation of many overlapping partial waves corresponding to the energetically allowed values of J tend to average the individual resonance signatures and still render them elusive to experimental observation.

Partial wave resonances were first observed for a few elastic collisions that involve simple atoms (*3*–*5*) and then for the F + HD → HF + D system. In this textbook three-atom reaction, the resonances could be identified by comparison of experimentally determined cross sections with the outcome of high-level electronic structure and quantum-scattering calculations. A clear oscillatory structure assigned to $J = 12$ to 14 partial waves appears in the collision energy dependence of the state and angle-resolved DCS (*6*), whereas a steplike feature characterizes the resonance behavior of the total ICS (*7*). More recently, resonance structures have been revealed in total ICSs for Penning ionization reactions of metastable He with H_2 or Ar in the cold regime (*8*) and in state-to-state ICSs for low-energy inelastic scattering of CO with H_2 (*9*). Yet, the identification of the contributing partial waves suffered from imperfect agreement with theory in the latter studies. Here, we report a joint experimental and theoretical study on O_2–H_2 inelastic collisions for O_2 ($N = 1$, $j = 0 \rightarrow N = 1$, $j = 1$) rotational excitation, a transition which violates the semiclassical propensity rules for rotational energy transfer involving a molecule in a $^3\Sigma$ state (*10*). The results demonstrate the purely quantum mechanical nature of the process and offer a complete characterization of fully resolved partial wave resonances with close agreement between theory and experiment.

We performed our experiments with a crossed-beam apparatus, which allowed us to tune the collision energy (the relative translational energy of colliding partners with reduced mass μ and relative velocity v_r) by varying the beam intersection angle, χ, between 12.5° and 90°: $E_T = \frac{1}{2}\mu v_r^2 = \frac{1}{2}\mu(v_{O2}^2 + v_{H2}^2 - 2v_{O2}v_{H2}\cos\chi)$ (*9*, *11*). H_2 and O_2 beams with low and matched velocities and high velocity resolution and quantum state purity were obtained by using cryogenically cooled Even-Lavie fast-pulsed valves (*12*) [see table S1 (*13*)]. Neat beams of *para*-H_2 and *normal*-H_2 were used and were characterized in the crossing region by 3 + 1 resonance-enhanced multiphoton ionization (REMPI) time-of-flight mass spectrometry using three-photon ($C^1\Pi_u$, $v = 0 \leftarrow X^1\Sigma_g^+$, $v = 0$) R branch transitions near 99,150 cm^{-1} (*14*). Populations >95% for $j = 0$ and <5% for $j = 1$ were deduced when using freshly prepared samples of *para*–H_2 and 25% $j = 0$, 75% $j = 1$ when using *normal*–H_2. The O_2 beam (0.3% O_2 in He) was probed by using 2 + 1 ($^3\Sigma_0^-$, $v = 2 \leftarrow X^3\Sigma_g^-$, $v = 0$) and ($^3\Sigma_1^-$, $v = 2 \leftarrow X^3\Sigma_g^-$, $v = 0$) REMPI transitions around 88,900 cm^{-1} (*15*). The relative populations of the three fine-structure components of ground rotational state $N = 1$ were estimated to be >85% in $j = 0$, <15% in $j = 2$ at $E_{1,2} = 2.08$ cm^{-1}, and <0.5% in $j = 1$ at $E_{1,1} = 3.96$ cm^{-1}, whereas those of first excited rotational state $N = 3$ were negligible (*13*). Cross-section measurements attributed to $N = 1$, $j = 0 \rightarrow N = 1$, $j = 1$ rotational energy transfer were performed by probing the collision-induced population in the $N = 1$, $j = 1$ level as a function of the crossing angle. The initial residual population in $N = 1$, $j = 1$ level was offset by shot-to-shot background subtraction when triggering the probe laser and the O_2 beam at 10 Hz with the H_2 beam at 5 Hz. The integral cross sections for O_2–*para*-H_2 collisions between $E_T = 3.7$ cm^{-1} and 20 cm^{-1} are displayed in Figs. 1A and 2. Those for O_2–*normal*-H_2 collisions are shown in Fig. 2. The excitation function displays well-

[1]Université de Bordeaux, Institut des Sciences Moléculaires, 33400 Talence, France. [2]CNRS, UMR 5255, 33400 Talence, France. [3]Laboratoire Ondes et Milieux Complexes, UMR 6294 CNRS–Université du Havre, 25 rue Philippe Lebon, BP 540, 76058 Le Havre, France. [4]Department of Optics and Spectroscopy, Tomsk State University, 36 Lenin av., Tomsk 634050, Russia. [5]Radboud University Nijmegen, Institute for Molecules and Materials, Heijendaalseweg 135, 6525 AJ Nijmegen, Netherlands.

*Corresponding author. E-mail: michel.costes@u-bordeaux1.fr (M.C.); francois.lique@univ-lehavre.fr (F.L.)

Science

Expanding the Fluorine Chemistry of Living Systems Using Engineered Polyketide Synthase Pathways

Mark C. Walker, Benjamin W. Thuronyi, Louise K. Charkoudian, Brian Lowry, Chaitan Khosla, and Michelle C. Y. Chang

Science, 341 (6150), • DOI: 10.1126/science.1242345

Stitching in Fluoroacetate

Polyketide synthase enzymes stitch together an impressively diverse series of organic compounds from simple acetate and propionate building blocks. Walker *et al.* (p. 1089) now show that these biochemical pathways can be engineered to incorporate fluoroacetate—a primary product of the only known native enzymatic fluorination route—into tri- and tetraketides. In *Escherichia coli* cells, this process shows potential as a versatile means of inserting fluorine substituents into a range of complex molecules for use in pharmaceutical and agrochemical research.

Science (ISSN 1095-9203) is published by the American Association for the Advancement of Science. 1200 New York Avenue NW, Washington, DC 20005. The title *Science* is a registered trademark of AAAS.